10.2478/v10170-011-0020-4

Archives of Control Sciences
Volume 22(LVIII), 2012
No. 2, *pages 191–215*

Comparison of two controllers for directional control of a hybrid electric vehicle

BASANTA KUMAR DASH and BIDYADHAR SUBUDHI

Directional response of a vehicle implies changing its direction when sustaining lateral acceleration while moving on the road. From this response, the vehicle's explicit capabilities as well as its contribution to the system performance of the driver/vehicle combination are obtained. In vehicle control literature, handling is often used interchangeably with cornering, turning, or directional response. This paper focuses one aspect of the handling i.e. directional response. Two different controllers, namely a PID controller and a Fuzzy Logic Controller (FLC) for a hybrid electric vehicle (HEV) are designed in this paper to control the vehicle's steering in a smooth lane change maneuver. The performances of the aforesaid two controllers have been studied extensively in this paper. For achieving an improved path tracking and directional response, parameters of both the PID and FLC have been tuned and their performances have been compared. Further, the effect of changing the scale factors in the fuzzy logic approach to obtaining directional response is presented. To validate the above two control performances, a nonlinear simulation model of a HEV is developed and is used in simulation studies. Both the controllers track the desired directional signal efficiently. Both PID and Fuzzy controllers provide competitive performances. Although with the assumption of all parameters of the vehicle available PID controller exhibits slightly better dynamic performance but in the real-world scenario the fuzzy controller is preferred due to its robustness i.e. it does not depend on the parameters of the vehicle.

Key words: directional control, active steering, fuzzy logic control, PID control, hybrid vehicle, four-wheel drive

1. Introduction

Developing a dynamic model of a vehicle moving on a road surface is important for designing controllers. Vehicles are usually subjected to acceleration, braking, ride and turning. Dynamic behavior is determined by the forces imposed on the vehicle from the tires, gravity and aerodynamics. The vehicle and its components are usually studied to determine forces produced by each of these sources at a particular maneuver and the vehicle response to these forces.

B.K. Dash is with Biju Patnaik University of Technology, Rourkela-769004, Odisha, India, email: bkdash.vidyog@gmail.com. B. Subudhi is with Department of Electrical Engineering, National Institute of Technology, Rourkela-769008, Odisha, India, e-mail: bidyadhar@nitrkl.ac.in

Received 22.04.2012. Revised 22.06.2012.

The objective of this paper is to develop a suitable control strategy for achieving improved directional response of a ground vehicle, thus improving the vehicle stability. Improving the vehicle stability will make the vehicle easier to handle. It will pay off in a reduced driver effort and so in an increased vehicle handling quality. Improving the vehicle stability will also reduce the chance for a driver to reach critical lateral driving conditions, such as extreme over steer or under steer. So basically, the development of the four- wheeled steering control strategy is in the scope of safe driving.

Automatic steering or directional control is an integral part of intelligent vehicle control system. The key objective of the directional controller is to perform automatic steering of the vehicle for tracking the steering command in order to track the driver's command in spite of changes in road conditions, wind and other disturbances, while maintaining good passenger comfort at all times. It includes tracking direction of the vehicle by translating driver's command into the corresponding steering angle command through rotational rate command.

The design of a directional control system, capable of controlling and coordinating the steering system for a four-wheel steering/drive (4WS) vehicle is a great challenge to the control system designer. Driver assistance systems for vehicle dynamics primarily produce a compensating torque for yaw disturbances. Such control systems can react faster and more accurately than the driver, when an unexpected deviation from the desired yaw rate occurs the deviation is taken between the desired yaw rate (generated by the function generator) and the actual yaw rate (measured by a rate sensor).

In recent years, the study of designing steering control systems for vehicles has attracted much attention of many authors [3, 7, 17] with the purpose of improving maneuverability and stability. Most of the vehicle models used to represent the dynamics were linear ones. Because of this, the control has to be restricted within small ranges of steering angle, and may not be appropriate to compensate for stability in critical motions.

In [6], it has been shown that feedback control can improve the robustness of the driver - vehicle system with respect to the uncertain operating conditions. It has been also reported in [6] that yaw rate feedback into front wheel steering is used to reduce the lateral displacements in an automatic steering system for a track-guided bus. In [6], the theory of unobservable/uncontrollable subspaces is used to improve the handling qualities of vehicles. Here front wheel steering command and yaw rate are unobservable from lateral acceleration. Here, the input is a step input only.

Reference [7] presents H_∞ control strategy of the active front wheel steering system to protect the vehicle spin and to realize the improved cornering performance where the mechanism of the vehicle spin behavior had been analyzed and explained using concepts of bifurcation theory. The linear H_∞ control theory has been applied to design a front wheel steering controller which compensates the instability against the nonlinear uncertainty [7]. The aerodynamic drag is a nonlinear function of the vehicle velocity and is highly dependent on weather conditions [16]. It is usually proportional to the square of the vehicle velocity and contributes 40% of the total force. In some of the research investigations [6, 7], the vehicle model has only two state variables yaw rate (ρ) and side slip angle (β) where as velocity (υ) has been taken as constant. So the effect of velocity

has been overlooked which is responsible for slip control and aerodynamic drag. The model also cannot be used for speed control to aid in directional or steering control.

PID control has been applied for directional control of a ground vehicle [1]. The performance of the PID controller deteriorates when the operating regime of the HEV deviates from nominal. Sometimes it becomes difficult for PID controller to provide accurate response because the model of the vehicle is uncertain. Subsequently to address model uncertainty, a FLC becomes a suitable selection for directional control of ground vehicles.

Fuzzy logic control has been implemented successfully in many industrial applications with significant performance improvement [10-14]. It has emerged as another methodology for the design of vehicle steering control system.

The operational parameters are based on terrain, traffic conditions, and driver requirements. In spite of slow varying assumption, the FLC has a difficulty in dealing with abrupt changes in the reference command; sharp turns, abrupt accelerations and breaking etc. The slow varying assumption may, however, come into play in the face of a continuing 'high frequency' input, due to the road surface or wind gust [1,18]. But slow-varying assumption allows the control law to adapt the changing conditions of wind, road surface etc.

Suitable yaw controller and speed controller can be designed in addition to directional controller, so that the entire vehicle state (ρ, υ, β) can be used to feedback to their respective controllers to aid steering or directional control [1].

In this paper, in the derived nonlinear model of the HEV, the yaw rate feedback to the front wheel steering has been also taken into consideration. Yaw rate, vehicle velocity and side slip are taken as state variables. Slow variation in the steering command is considered in this work.

The rest of the paper is organized as follows. The directional dynamics of the vehicle is described in section 2. Section 3 presents the design aspects of two controllers namely PID and Fuzzy controllers applied for the directional control of the HEV. Implementation, results and discussions are presented in section 4. Finally, conclusions are provided in section 5.

1.1. Vehicle directional dynamics

Schematic diagram of a HEV is shown in Fig. 1. The vehicle and its components are studied to determine forces produced by each of these sources at a particular maneuver and the vehicle response to these forces. A ground vehicle in a turning maneuver is modeled. During such a lane-change maneuver, the vehicle undergoes translational as well as rotational motion. When modeling a moving vehicle, it is convenient to use a reference coordinate frame attached to and moving with the vehicle. This is because with respect to the vehicle coordinate frame, moment of inertial of the vehicle is constant. The dynamics of the vehicle can be described by choosing three states yaw rate (ρ), velocity vector (υ) and side slip angle (β) while the controlled inputs are the front and (optionally)

rear wheel steering angles δ_f and δ_b respectively and the nonlinear model that is derived in this section shortly.

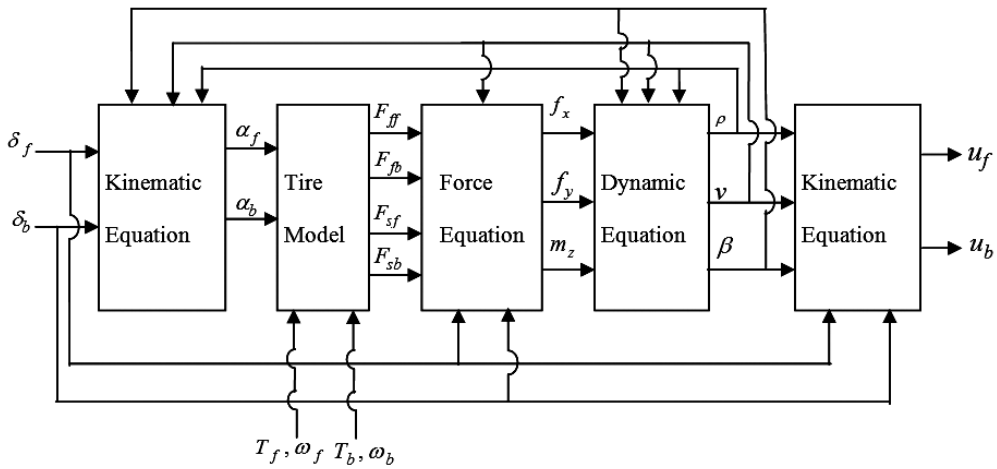

Figure 1. Schematic diagram of a HEV.

On-board, the vehicle motions are defined with reference to a right-hand orthogonal coordinate system (the vehicle fixed coordinate system) which originates at the center of gravity (CG) and travels with the vehicle. Following the SAE (Society of Automotive Engineers) convention, the x-coordinates directed forward and on the longitudinal plane of symmetry of the vehicle, y-coordinate is the lateral direction out the right hand side of the vehicle and z-coordinate is directed down-ward with respect to the vehicle. In rotational motions, p is the roll velocity about the x-axis; q is the pitch velocity about the y-axis and ρ is the yaw velocity about the z-axis.

Vehicle motion is usually described by the velocities (forward, lateral, vertical, roll, pitch and yaw) with respect to the vehicle fixed coordinate system, where the velocities are referred to the earth fixed coordinate system.

Vehicle attitude and trajectory through the course of a maneuver are defined with respect to a right-hand orthogonal axis system fixed on the earth. It is normally selected to coincide with the vehicle fixed coordinate system at the point where the maneuver is started. x_0, y_0 and z_0 are the coordinates of earth fixed or global or absolute coordinate system representing forward travel, travel to the right, and vertical travel (positive down ward) respectively. This coordinate system is used in this paper.

The essential feature of the vehicle steering dynamics in a horizontal plane are described by the 'single-track model' (or 'two-wheel model' or 'bicycle model') [2]. Since the objective in this paper is to compare and evaluate the performance of the directional controllers for the HEV, a number of assumptions in modeling the HEV are taken. A two-wheel 'bicycle' model for the chassis rather than a full four-wheel model is con-

sidered. The 'bicycle' model preserves the dynamics of the full four-wheel HEV, while significantly reduces the complexity of the vehicle simulation model [1].

To develop a simple model, the effects of roll and pitch are neglected. The origin of the vehicle coordinate system is located at the vehicle CG. It may be noted that, acceleration, braking, and most turning analysis, one mass is sufficient. For single mass representation, the vehicle is treated as a mass concentrated at its CG , the point mass at CG (m), with appropriate rotational moment of inertia (I), is dynamically equivalent to the vehicle itself for all motions in which it is reasonable to assume the vehicle to be rigid.

The bicycle or single track model is a relatively simple vehicle model. However, it is used quite often in studies on 4WS to assess the potential of steering strategies. The bicycle model is a mathematical model of a two-wheel in-plane vehicle. The following assumptions apply to the bicycle model:

1. The CG is assumed to be midway between the front and rear axles of the vehicle.

2. The CG is assumed on the road level such that there is no coupling from pitch and roll motions. Hence body roll and pitch are not taken into account. So the normal force exerted from the ground on to the wheels is constant.

3. For a single mass representation, the vehicle is treated as a mass concentrated at the CG. The point mass at CG (m), with appropriate I, is dynamically equivalent to the vehicle itself for all motions in which it is reasonable to assume the vehicle to be rigid. The mass of the vehicle is assumed to be concentrated at the front and back wheels with total mass, m.

4. The vehicles chassis is assumed to be directed in the x-direction relative to the $x-y$ coordinate system which is translated by an angle ψ from an absolute x_0-y_0 coordinate system.

5. The left and right tire characteristics are lumped into an equivalent tire characteristic, which describes the axle's lateral tire force as a function of the slip angle.

6. The lateral tire forces are proportional to the slip angles of the tires under the assumption that the slip angles are small. The proportionality constant is called the cornering stiffness C.

7. The longitudinal mass distribution be equivalent to concentrated masses at the front and rear axles. Then the total mass m is related to I with respect to a perpendicular axis through CG by $I = ml_f l_b$.

8. The vehicle is symmetric about $x-z$ plane.

Fig.2 depicts the bicycle model of a vehicle. The variables of this model are given in Tab. 1.

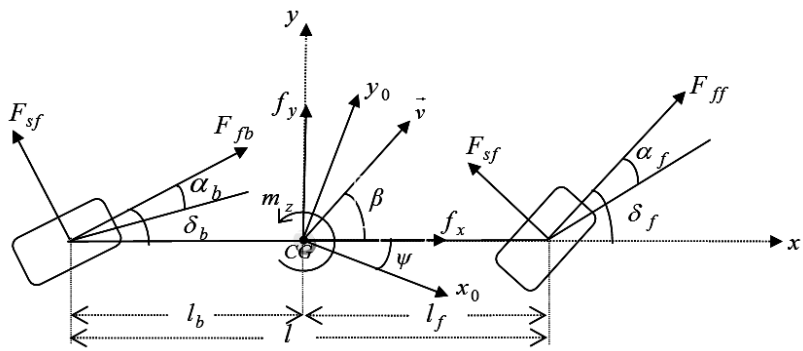

Figure 2. Bicycle model.

The bicycle model is obtained by lumping the two front wheels into one wheel in the centerline of the vehicle. The same is done with the two rear wheels (see Fig. 2). In Fig. 2, $\overrightarrow{v}$ is the velocity vector at the CG. It has the absolute value $v = |\overrightarrow{v}|$. It is assumed that $v > 0$ because the vehicle is not controllable for $v = 0$. The distance between CG and front axle (rear axle) is $l_f(l_b)$ and the sum $l = l_f + l_b$ is the wheel base. The angle β between centerline and velocity vector is called 'side slip angle'. In the horizontal plane of Fig. 2 an absolute coordinate system (x_0, y_0) is shown together with a vehicle fixed coordinate system (x, y) that is rotated by a 'yaw angle' ψ.

The dynamics of the vehicle model is described by the following set of equations. The front and rear tire slip angles respectively are derived from the chassis kinematics are as follows.

$$\alpha_f = \delta_f - \tan^{-1}\left(\tan(\beta) + \frac{l_f \rho}{v\cos(\beta)}\right), \tag{1}$$

$$\alpha_b = \delta_b - \tan^{-1}\left(\tan(\beta) - \frac{l_b \rho}{v\cos(\beta)}\right). \tag{2}$$

Similarly, expressions for the speed of the front and rear wheel respectively in the plane of the wheel are derived from chassis kinematics as follows.

$$u_f = v\cos(\delta_f - \beta) + l_f \rho \sin(\delta_f), \tag{3}$$

$$u_b = v\cos(\delta_b - \beta) + l_b \rho \sin(\delta_b). \tag{4}$$

The dynamic equations of the vehicle are obtained from force equations of the vehicle such as translational motions along x and y axes and rotational moment about vehicle CG. The translational and rotational dynamics for the HEV chassis is given by

$$m\dot{v} = f_x \cos(\beta) + f_y \sin(\beta), \tag{5}$$

$$mv\left(\dot{\beta} + \rho\right) = -\sin(\beta) f_x + \cos(\beta) f_y, \tag{6}$$

Table 1. Variables used in the chassis model.

$x-y$	vehicle coordinate system
x_0-y_0	earth fixed or absolute or global coordinate system
g	gravitational constant (m/sec^2)
l	wheel base (m) (length of the vehicle measured between its front and rear axles)
l_i $i=\{f,b\}$	distance between the front/rear axle and the center of gravity of the vehicle (m)
m	mass of the vehicle (kg) $(m=m_f+m_b)$
m_i; $i=\{f,b\}$	the mass concentrated on the front/rear axle of the vehicle (kg) $\left(m_b=\frac{ml_f}{l}, m_f=\frac{ml_b}{l}\right)$
β	vehicle side slip (rad) (the angle between the vehicle velocity vector and its centerline)
ψ	angle between the vehicle centerline and the absolute x_0-y_0 coordinate system (rad)
ρ	yaw rate (first derivative of the angle between the vehicle centerline and the absolute x_0-y_0 coordinate system, (rad/sec) $(\rho=\dot{\psi})$
δ_i; $i=\{f,b\}$	front/rear steering angle (rad)
α_i; $i=\{f,b\}$	side slip of the front/rear wheel (rad) (the angle between the velocity vector of the front/rear wheel and the centerline of the wheel)
θ	inclination of the road (rad)
f_x	translation force on the vehicle chassis in the x direction (N)
f_y	translation force on the vehicle chassis in the y direction (N)
m_z	rotational moment on the vehicle chassis about the center of gravity (kg·m^2)
F_{fi}; $i=\{f,b\}$	total forward force on the front/rear wheel (N)
F_{si}; $i=\{f,b\}$	total side force on the front/rear wheel (N)
u_i; $i=\{f,b\}$	speed of the front/rear wheel in the plane of the wheel (m/sec)
v_i; $i=\{f,b\}$	speed of the front/rear wheel (m/sec)

$$ml_f l_b\dot{\rho}=m_z, \tag{7}$$

where f_x and f_y are the translational forces on the vehicle chassis in the x and y direction. m_z is the rotational moment about the vehicle's center of gravity. These forces are

computed from the total tire forces F_{ff}, F_{fb}, and F_{sf}, F_{sb} and the external forces on the vehicles. External forces are F_{ex} in the x direction while the external forces in the y direction are taken to be zero, together with the vehicle kinematics. Here the external forces include aerodynamic drag and gradient resistance due to the inclination of the road.

Total longitudinal force (f_x) is given by summing the forces along the x axis and described as

$$f_x = F_{ff}\cos(\delta_f) + F_{fb}\cos(\delta_b) - F_{sf}\sin(\delta_f) - F_{sb}\sin(\delta_b) - F_{ex} \tag{8}$$

where F_{ex} is the external forces such as aerodynamic drag and gradient resistance acting on the vehicle given by

$$F_{ex} = \text{Aerodynamic Drag}\left(\frac{1}{2}\left(C_d\rho_a + Av^2\right)\right) + \text{Gradient Resistance}\left(mg\sin(\phi)\right). \tag{9}$$

Total lateral force (f_y) is given by summing the forces along the y-axis described as

$$f_y = F_{sf}\cos(\delta_f) + F_{sb}\cos(\delta_b) + F_{ff}\sin(\delta_f) + F_{fb}\sin(\delta_b). \tag{10}$$

The equation of yaw motion is obtained by summing the torques with respect to the z axis.

$$m_z = l_f F_{ff}\sin(\delta_f) - l_b F_{fb}\sin(\delta_b) + l_f F_{sf}\cos(\delta_f) - l_b F_{sb}\cos(\delta_b) \tag{11}$$

where m_z is the rotational moment on the vehicle chassis about the CG.

The nonlinear forces F_{ff}, F_{fb} are the front and rear forward forces respectively and F_{sf}, F_{sb} are the front and rear side forces respectively which can be determined from the wheel dynamics.

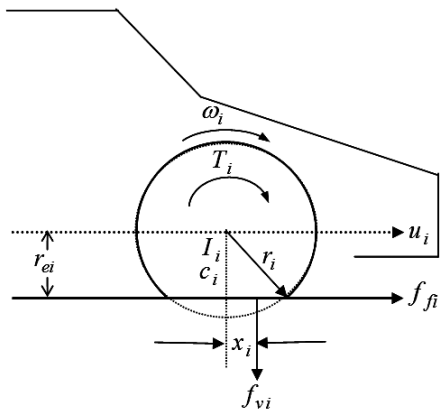

Figure 3. Wheel dynamics geometry.

The wheel dynamics model is derived that is based on the geometry illustrated in Fig. 3 and is summarized in Tab. 2. The deformation of the rubber tire due to gravity and the forces on the wheel has been taken into account [4]. So, the equations describing

Table 2. Variables used in the wheel model

ω_i; $i = \{f,b\}$	rotational speed of the front/rear wheel unit (rad/sec)
T_i; $i = \{f,b\}$	torque applied to the front/rear wheel by its motor/generator (N-m)
r_i; $i = \{f,b\}$	radius of the front/rear wheel (m)
r_{ei}; $i = \{f,b\}$	effective radius of the front/rear wheel(m)
x_i; $i = \{f,b\}$	offset from the center of the front/rear wheel where the vertical force is concentrated(m)
f_{fi}; $i = \{f,b\}$	forward tire force produced by the front/rear wheel(N)
f_{si}; $i = \{f,b\}$	side tire force produced by the front/rear wheel(N)
f_{yi}; $i = \{f,b\}$	vertical force produced by the front/rear wheel(N)
s_i; $i = \{f,b\}$	tire slip ratio of the front/rear wheel
c_i; $i = \{f,b\}$	tire wear/road surface condition parameter for the front/rear wheel
I_i; $i = \{f,b\}$	moment of inertia of the front/rear wheel unit (kg·m^2)
ζ_i; $i = \{f,b\}$	damping coefficient of the front/rear wheel unit
μ_i; $i = \{f,b\}$	adhesion coefficient

wheel dynamics includes effective radius of the wheel (r_{ei}) and offset (x_i) from the center of the wheel where the vertical force is concentrated.

The tire force functions are highly dependent on the tire and road conditions. However, these forces must be balanced by the forces applied to the wheel through the chassis. The forward and side forces on the wheel are function of the wheel slip (λ) and tire slip ratio (s). The tire slip ratio which is a measure of the degree to which ith tire is spinning on the road surface due to ice, worn tire tread etc, is given by

$$s_i = 1 - \frac{u_i}{\omega_i r_{ei}}; i = \{f,b\}. \tag{12}$$

The total forward force on the wheel includes the force due to motor-generator torque, the motor-generator-wheel unit inertia, wheel damping and the vertical force offset in addition to forward tire force. The total forward force acting on the wheel is

$$F_{fi} = \frac{1}{r_{ei}} \left[T_i + f_{vi} x_i - c_i f_{fi} r_{ei} - I_i \dot{\omega}_i - \zeta_i \omega_i \right]; i = \{f,b\}. \tag{13}$$

Since f_{si} is the only side force acting on the wheel, the total side forces acting on the wheel are

$$F_{si} = c_i f_{si}; i = \{f,b\} \tag{14}$$

where c_i is the tire-wear-road surface condition parameter which characterizes the percentage of tire force which actually applied to the road surface. For the case a dry road

and good tire condition, the value of $c_i = 1$ and for the case of icy road and/or extreme case of worn tires, the value of $c_i = 0$ where none of the tire forces applied to the road surface. Hence the value of c_i varies between 0 and 1. The tire forward force and side force acting on the wheel for a typical passenger car, are calculated from the forward and side force function shown in Fig. 4 [1] and Fig. 5 [4] respectively.

$$c_{\alpha i} = \frac{df_{si}}{d\alpha}; i = \{f, b\}, \tag{15}$$

$$f_{sf} = c_{\alpha f}\alpha_f \quad \text{and} \quad f_{sb} = c_{\alpha b}\alpha_b. \tag{16}$$

HEV model is obtained by combining the above equations where ρ, υ and β are the state variables of the HEV model. δ_f and δ_b are the inputs to the dynamic model, while T and ω are outputs of the motor which serve as inputs to the chassis dynamic model.

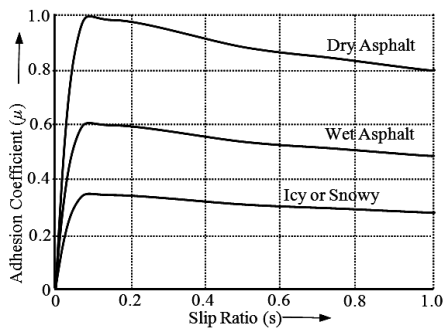

Figure 4. Typical adhesion coefficients (μ) versus slip ratio(s) curve [9].

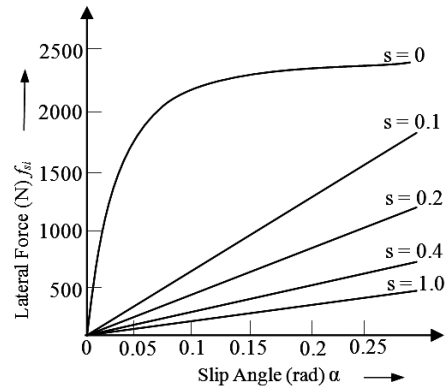

Figure 5. Typical cornering characteristics [4].

2. Directional controllers design

Fig. 6 shows the structure of a directional vehicle control system. The control objective is to minimize the error between the reference yaw rate (ρ_{ref}) and the actual yaw rate (ρ).

The directional controller architecture basically consists of three blocks, namely vehicle dynamics block represented by equations (1) to (16), directional control block consisting either PID controller or fuzzy controller with an integrating actuator to enhance the directional performance of the vehicle, and a reference signal generator which smooths the step steering angle input from the driver to change the vehicle maneuver from step or sudden lane change to smooth lane change. The reference signal generator block is absent in the study of directional response of the vehicle in step or sudden lane change maneuver.

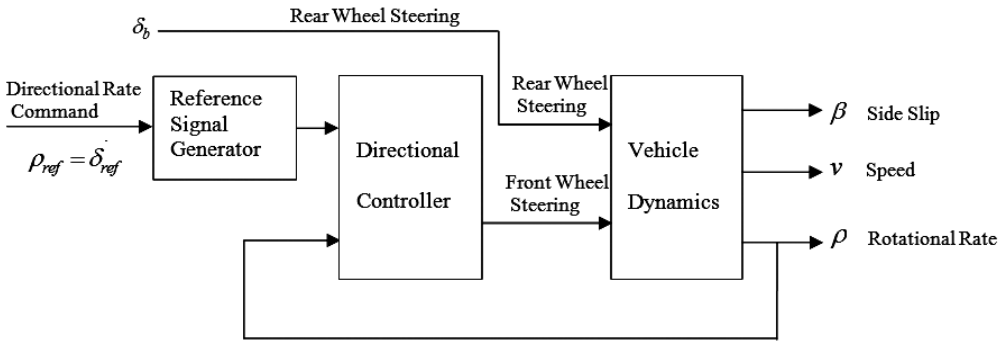

Figure 6. Architecture of directional controller.

The driver's input is translated into the corresponding steering angle command through rotational rate command (ρ_{ref}) [6]. The steering response of a vehicle depends on uncertain mass, road condition and velocity. Robustness can be achieved by controlling the yaw rate instead of the steering angle. [6]. Integrating unit feedback of the yaw rate error makes the yaw mode unobservable from the front axle lateral acceleration and thereby takes uncertainty out of the steering transfer function [6]. The yaw rate (ρ) and the steering wheel angle is used as a reference input ρ_{ref} for ρ. The error signal, $\rho_{ref} - \rho$ is processed by a directional controller that controls the actuator for the steering angle. δ_f is generated by an integrating actuator, e.g. a hydraulic or electric motor without servo feedback loop.

Sensing state variables of the vehicle dynamics is not only difficult but also challenging. For directional control of the HEV, the output variable of interest is yaw rate (ρ) which can be sensed with a gyroscope. Sensing of other two variables, υ and β is relatively more difficult than the first one. β can be readily derived from the vehicle's vector velocity but the main problem is sensing vehicle's vector velocity (υ). A method has been proposed of sensing vehicle's vector velocity by combination of lookdown sensor, high resolution GPS, and accelerometers [1] because only lookdown sensor which is the most promising and low cost sensor has the difficulty on ice or watery road. It can be noted here that tire slip is treated as part of vehicle dynamics.

In this section, two controllers namely a PID and fuzzy controller design for achieving directional control is described.

2.1. PID based directional controller

The PID control law is given by

$$u(t) = k_p + k_i \int_0^t e(\tau)d\tau + k_d \frac{d}{dt} e(t) \tag{17}$$

where $e(t)$ is the yaw rate error, is the deviation of the vehicle from the desired steering command, given by $e(t) = \rho_{ref} - \rho$. k_p is the proportional gain, k_i is the integral gain and k_d is the derivative gain of the PID controller. Based on the yaw rate deviation, the servo correction is done using PID algorithm. The steer is linear only for a certain interval of error after which it varies non-linearly. In order to attain linearity, integral and derivative controllers are considered along with proportional.

When the vehicle deviates from the desired path to right (left), then error must be accumulated. When the vehicle moves from right (left) to the desired path, error must be subtracted from the accumulated value so as to bring back the vehicle to the line of desired path. This is accomplished by comparing present error with the previous error.

2.2. Fuzzy logic based directional controller

The operational parameters of a ground vehicle are based on terrain, traffic conditions, and driver requirements which are uncertain as a result of which the vehicle undergoes abrupt changes in the reference command; sharp turns, abrupt accelerations and braking etc. So to address these uncertainties, a FLC becomes a suitable choice for directional control of ground vehicles. A PD type FLC for controling the rotational rate of the HEV is designed. A PD FLC is chosen because a PD-FLC gives a faster transient response than a PI-FLC. The structure of a typical PD-FLC for the HEV model is depicted in Fig. 7.

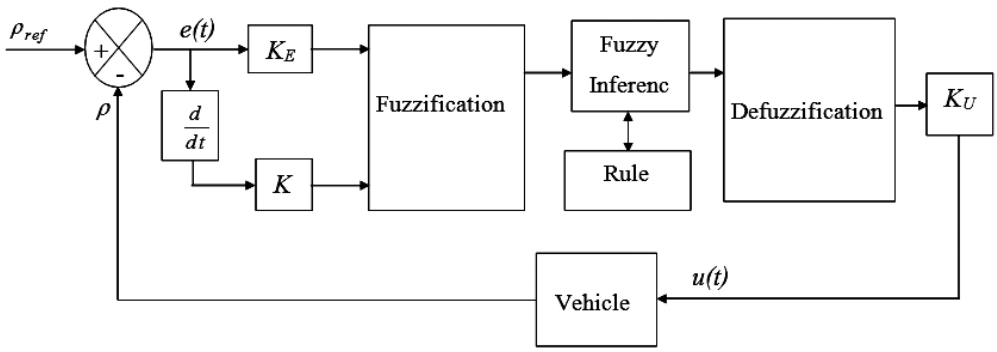

Figure 7. Structure of the PD-FLC.

Error (e) and the rate of change in the control error (ce) are chosen as the inputs for the FLC whilst $u(t)$ as the output variable. The error and change in error is defined as

$$e(t) = \rho_{ref} - \rho \quad \text{and} \quad \dot{e}(t) = \dot{\rho}_{ref} - \dot{\rho}. \tag{18}$$

In order to aid in faster computation, the input normalization block transforms the input variables e and ce from actual universe of discourse (UOD) (E and CE) to the normalized universe of discourses E_n and CE_n (e_n and ce_n) in the range (-1.0 to 1.0),

using the input scale factors K_E and K_{CE}. Their scale factors are defined as follows.

$$K_E = \frac{e_n}{e}, K_{CE} = \frac{ce_n}{ce} \quad \text{and} \quad K_U = \frac{u_n}{U} \tag{19}$$

The fuzzification block converts crisp values of inputs variable to appropriate fuzzy sets embedding membership functions as shown in Fig. 8(a), 8(b) and 8(c). Three symmetric triangular fuzzy sets, N (negative), Z (zero) and P (positive), are chosen for both the input variables and five symmetric triangular fuzzy sets, NB (negative big), N (negative), Z (zero), P (positive) and PB (positive big), are chosen for the output variable. The information of the membership function shapes the linguistic control rules and fuzzy compose the knowledge base of the FLC. The fuzzy inference engine performs fuzzy reasoning, based on the fuzzy rules, using Zadeh's compositional rule of inference given by

$$U = (E \times CE) \circ R \tag{20}$$

where R is the fuzzy rule, $\times$ is the cartesian product and $\circ$ is the sup-min operation. The control action U(u_i) for the ith rule can be obtained using the following inferencing

$$U(u_i) = \left\{E(e_j) \cap CE(\dot{e}_k) \cap R_{jk}(e_j, \dot{e}_k, u_i)\right\} \tag{21}$$

and a maximum operation is performed over all the rules to find the fuzzy control vector as

$$U(u) = \underset{i=1,\ldots,n}{U} \left\{E(e_j) \cap CE(\dot{e}_k) \cap R_{jk}(e_j, \dot{e}_k, u_i)\right\} \tag{22}$$

where $n(n = jl)$ is the number of rules.

The antecedent indices j and k respectively for $E(e_j)$ and $CE(\dot{e}_k)$ in the rule base are used to access the corresponding consequent $U(u_i)$ for the ith rule, R_i (which is the same as R_{jk}).

The defuzzification block transforms the crisp control output $u(t)$ from the inferred membership values of $\mu_U(u)$ by the popular centre of gravity method of defuzzification that is given as

$$u(t) = \frac{\sum_{i=1}^{n_r} \mu_i(u) u_i}{\sum_{i=1}^{n_r} \mu_i(u)} \tag{23}$$

where u_i is the centroid and $\mu_i(u)$ is the membership function value of the fuzzy set for the consequent (control action in this case) inferred at the ith quantization level on the control space (UOD); n_r is the number of quantization intervals. Just like input normalization, the output (u_n) in the computational UOD (U_n) is denormalized by using the scaling factor K_U to obtain the control action $u(t)$ in the actual UOD (U).

The first priority is to tune the scaling factors, because these are the global tuning parameters that affect the overall control performance. In adjusting these , consideration is given to rise time (t_r), overshoot (M_p) and the steady state error. When the response is

far away from the desired value, the input scaling factors are adjusted to reduce the rise time, and later readjusted to prevent overshoot as the response approaches the desired value. The output scaling factor is tuned to limit the FLC output to a reasonable value and to reduce the steady state error (e_{ss}).

Selection of appropriate fuzzy control rules is essential for obtaining efficient performance of the FLC. Several methods of deriving appropriate if-then fuzzy rules could be used [10], but this paper uses an error plane method [11]. The error response plane method is effectively a fuzzy logic control version of the well known sliding mode controller. Here in the FLC, 9 rules were constructed which are shown in Tab. 3.

Here the input signal is $u = \delta_f$ (the front wheel steer angle) and $\delta_b = 0$ [6]. The range of error (e) and change of error (ce) are [-0.5, 0.5] and [-0.06, 0.06] respectively. The range for the controller output is [-3^0, 3^0]. The rule matrix is shown in Tab. 3. The membership functions for the error, the change in error, and controller's output are shown in Fig. 8(a), 8(b) and 8(c), respectively.

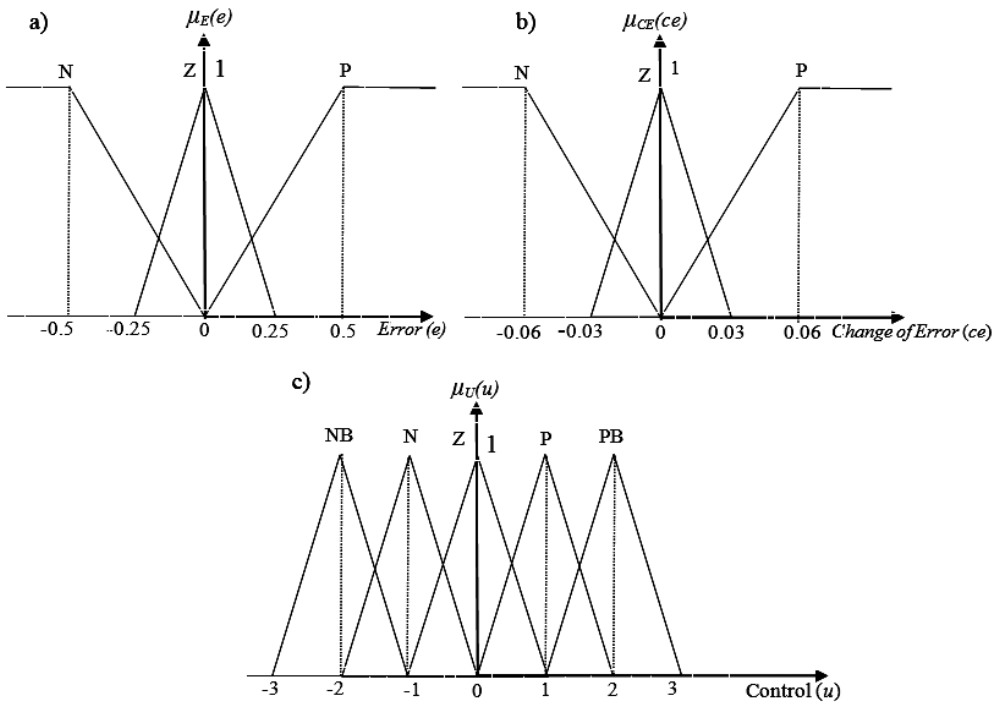

Figure 8. Membership functions: a) error (e), b) change of error (ce), c) control (u).

Table 3. Rule base matrix.

		Change in Error (ce)		
		P	Z	N
Error (e)	P	PB	P	Z
	Z	P	Z	N
	N	Z	N	NB

3. Implementation, results and discussion

The vehicle's directional control using PID and fuzzy as discussed in section 3 was implemented using MATLAB/SIMULINK. The parameters of the vehicle used for the simulation are given in Tab. 4

Table 4. HEV simulation parameters.

No load weight of the vehicle	1100 kg
Air density	1.225 kg/m^3
Vehicle wheel base	2.6 m
Aerodynamic drag coefficient	0.4
Distance between CG and front axle	1.3 m
Inclination of the road	15 degrees
Distance between CG and rear axle	1.3 m
Applied tractive torque	300 Nm
Vehicle cross section	2.3 m^2
Rotational speed of the wheel	300 rpm
Wheel radius	0.30 m
Adhesion coefficient	0.9
Effective wheel radius	0.27 m
Slip of the wheel	0.2
Moment of inertia	1.6 kg·m^2
Stiffness coefficient	10000 N/rad
Viscous damping	0.17 m·kg·sec

3.1. PID controller

The gains k_p, k_i, and k_d have been tuned for the HEV with no load on a dry road. These gains of the PID controllers are given in Tab. 5. The parameters used for the HEV model in these simulations are given in Tab. 4. The directional response has been studied for both smooth lane change maneuver as well as step lane change maneuver. For smooth lane change maneuver, a reference function generator with step input has been taken which produce reference rotational rate command. For step lane change maneuver, a step function of 0.1 radian (18 degrees) has been taken for a dry road without loading condition of the vehicle. In both the cases the tracking efficiency to the directional command has been simulated by using MATLAB/SIMULINK (Fig. 9). In all simulations, the simulation time was set as 35 seconds.

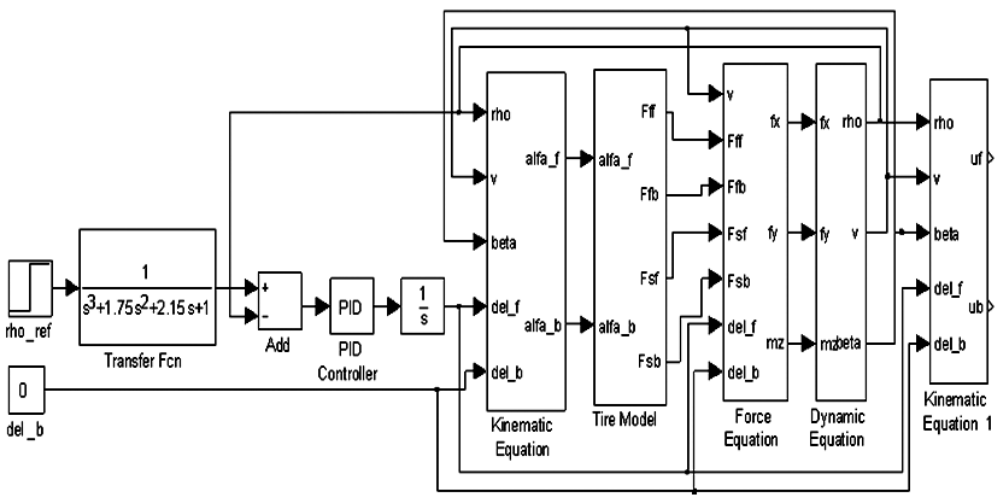

Figure 9. SIMULINK implementation of the PID directional controller for HEV.

Table 5. Gains of the PID controller.

k_p	k_i	k_d
10	2	25

Fig. 10 (a) and 10 (b) (which is an enlarged version of Fig. 10 (a)) shows the effect of PID control when there is a smooth lane change. It is seen from this figure that when control is applied the rotational rate (ρ) response is oscillatory with maximum overshoot 2% but with a PID control the maximum overshoot is reduced to 1.5% which improves the ride comfort. With PID control the steady state error becomes zero and settled in

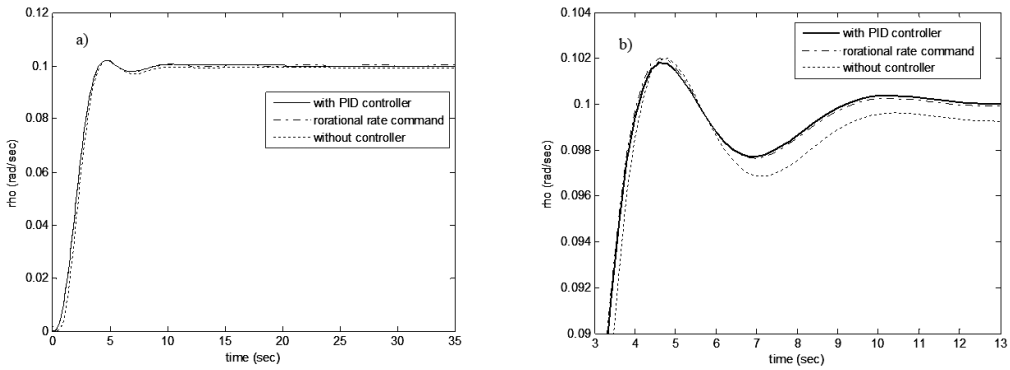

Figure 10. Comparison of directional response with and without PID controller in a smooth lane change maneuver.

Table 6. Comparisons of controllers' performance.

Lane change maneuver	Without Controller				PID Controller			
	t_r (sec)	t_s (sec)	M_p (%)	SSE (%)	t_r (sec)	t_s (sec)	M_p (%)	SSE (%)
Smooth lane change	4.25	Infinity 10 (1% t_s)	2	1	4	9	1.5	0

Lane change maneuver					Fuzzy Logic Controller			
					t_r (sec)	t_s (sec)	M_p (%)	SSE (%)
Smooth lane change					4.5	9	2	0

9 sec whereas without control there is 1% steady error and with this error settling time is 10 sec.

3.2. A fuzzy logic controller

The error and change of error are scaled by 1000 and 1 respectively for fast and simple calculations. Similarly the output is scaled by the factor $\frac{2\pi}{180}$ before using it as the vehicle's steering input. The factor $\frac{2\pi}{180}$ converts degree into radians. To increase the control input signal, 2 is multiplied which allows us to use the same controller to track step inputs with large amplitudes. A plot of the control surface is given in Fig. 13. The transfer function used as the signal generator is given by $\frac{1}{s^3+1.75s^2+2.15s+1}$. The closed loop system is simulated using SIMULINK (Fig. 11).

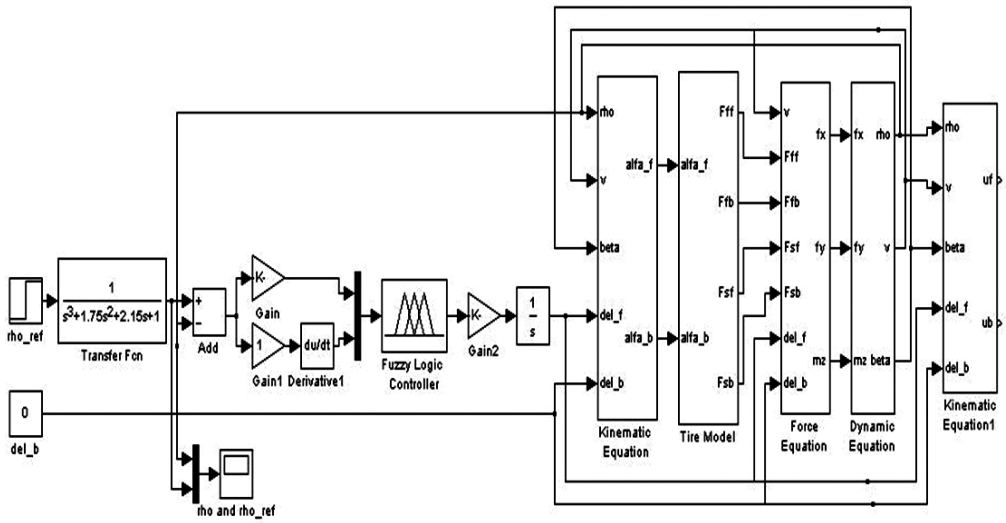

Figure 11. SIMULINK implementation of the fuzzy logic directional controller for HEV.

The best values chosen for the scale factor for fuzzy logic controller are $K_E = 1000$, $K_{CE} = 1$ and $K_U = 2\pi/180$. A comparative assessment of the PID and FLC performances for directional control of the HEV is presented in Tab. 6. The effect of variation of different scale factors on directional response of the HEV are shown in Tab. 7, 8 and 9.

Table 7. Effect of variation of K_E on stability and steady state error when $K_{CE} = 1$ and $K_U = 2\pi/180$ in a smooth lane change maneuver.

K_E	SSE (in %)	Stability	Remarks
0.01 0.001 0.0001	- infinity	unstable	All three has similar response characteristics
0.1	infinity	unstable	Increases gradually linearly and become unstable with infinite steady state error
1	10	stable	
10	1	stable	
100	0.1	stable	
1000	0.01	stable	99.99% accuracy

The effect of variation of K_E on stability and steady state error when $K_{CE} = 1$ and $K_U = 2\pi/180$ in a smooth lane change maneuver is given in Tab. 7. For $K_E = 1$, the

Table 8. Effect of variation of K_{CE} on stability and steady state error when $K_E = 1000$ and $K_U = 2\pi/180$ in a smooth lane change maneuver.

K_{CE}	SSE (in %)	Stability	Remarks
100	100	stable	Rise time is 4 sec, peak value is 0.01. Response comes to zero in 204 sec.
5			Model error.
2	100	unstable	Response gradually increases and becomes unstable with 100% steady state error.
4, 6, 7, 8, 9, 10, 20, 50			Simulation is not complete.
3, 1, 0.1, 0.01	0.01	stable	Perfectly tracking.

Table 9. Effect of variation of K_U on stability and steady state error when $K_E = 1000$ and $K_{CE} = 1$ in a smooth lane change maneuver.

K_U	Stability	SSE (in %)	Remarks
$(n\pi/180)$ for $n = 0.5, 1, 2, 3, 6, 7$ $8, 10, 13, 14, 15$ $16, 17, 18, 20$	stable	0.01	Perfectly tracks but for $n = 7$ and 10, some intermediate disturbance occurs
$(n\pi/180)$ for $n = -1, -2, -3, -4$	stable	100	Response becomes zero
$(n\pi/180)$ for $n = 4, 5, 9, 12, 16, 19$			Model error
$11\pi/180$	unstable	infinity	Perfectly tracks up to 5 sec and then falls gradually linearly and becomes unstable
$(\pi/n180)$ for $n = 3, 4, 5, 6, 7, 8, 9, 10$	stable	100	Response becomes zero but when n increases the peak response decreases

Table 10. Effect of variations of K_E, K_{CE} and K_U on dynamic directional response in a smooth lane change maneuver.

Scaling factors	Variations	Stability	Steady state error (e_{ss})	Settling time (t_s)	Remarks
K_E	increases	improves	decreases	decreases	
K_{CE}	increases	decreases	increases	increases	
K_U	+ve increases	unaffected	unaffected		
K_U	-ve increase	stable	100%		steady state response is zero
K_U	decreases	stable	100%		steady state response is zero with decreasing peak value

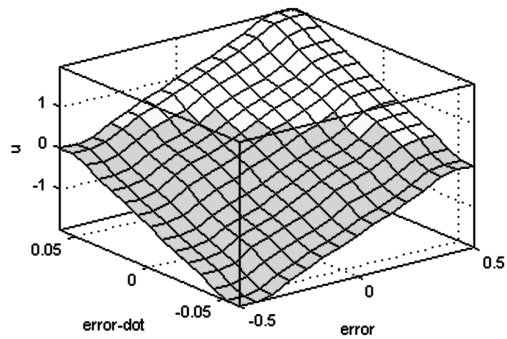

Figure 12. Plot of the control surface $u = f(e, ce)$.

response is stable with 10% steady state error, shown in Fig. 16. When K_E decreases the system becomes unstable with infinite error which is shown from Fig. 17 $(K_E = 0.1)$, Fig. 19 $(K_E = 0.01)$. When K_E increases, the steady state error decreases and the dynamic response tracking the yaw rate command improves. For $K_E = 10$, $K_E = 100$, $K_E = 1000$ the directional responses are shown in Fig. 15, Fig. 14, Fig. 13 respectively are stable with steady state errors of 1%, 0.1% and 0.01% respectively.

The effect of variation of K_{CE} on stability and steady state error of directional response when $K_E = 1000$ and $K_U = 2\pi/180$ in a smooth lane change maneuver is shown in Tab. 8. The directional response for different value of K_{CE} are shown in Fig. 19, Fig. 20, Fig. 21 and Fig. 22. For $K_{CE} = 2$, the response increases up to 1 in 23 seconds and then falls and becomes stable with zero steady state error shown in Fig. 21. For $K_{CE} = 5$,

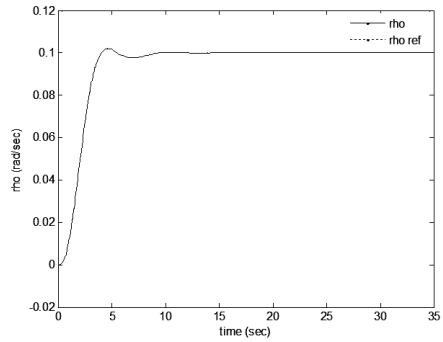

Figure 13. $K_E = 1000$, $K_{CE} = 1$, $K_U = 2\pi/180$.

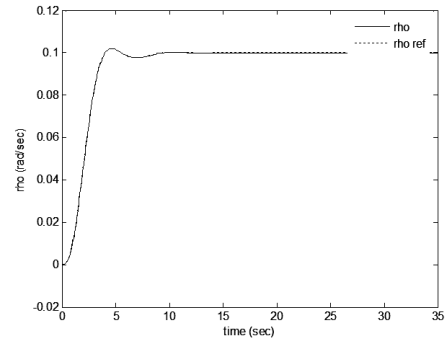

Figure 14. $K_E = 100$, $K_{CE} = 1$, $K_U = 2\pi/180$.

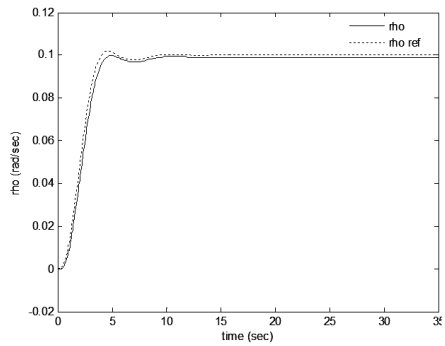

Figure 15. $K_E = 10$, $K_{CE} = 1$, $K_U = 2\pi/180$.

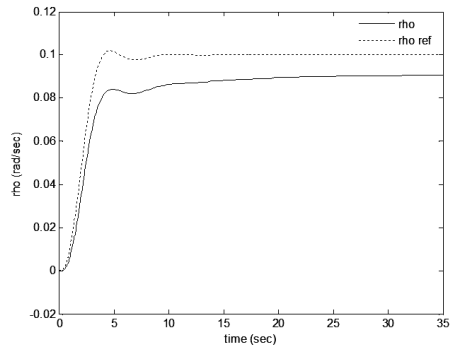

Figure 16. $K_E = 1$, $K_{CE} = 1$, $K_U = 2\pi/180$.

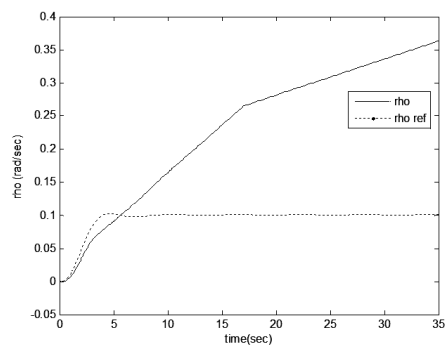

Figure 17. $K_E = 0.1$, $K_{CE} = 1$, $K_U = 2\pi/180$.

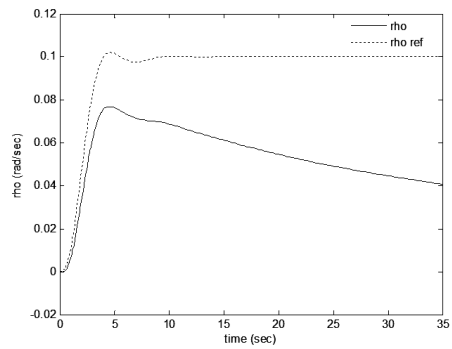

Figure 18. $K_E = 0.01$, $K_{CE} = 1$, $K_U = 2\pi/180$.

the directional response gradually increases linearly and becomes unstable shown in Fig. 22. For $K_{CE} = 100$, the directional response only attains its peak value as 10% of the steady state value in 4 seconds and then falls slowly in sluggish manner and becomes

zero in 204 seconds shown in Fig. 23. For $K_{CE} = 1$, the directional response perfectly follows the yaw rate command with 99.99% accuracy which is shown in Fig. 14.

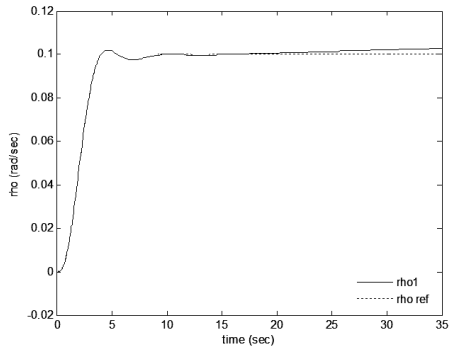

Figure 19. $K_E = 1000$, $K_{CE} = 3$, $K_U = 2\pi/180$.

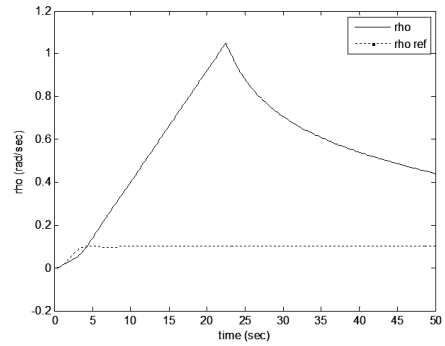

Figure 20. $K_E = 1000$, $K_{CE} = 2$, $K_U = 2\pi/180$.

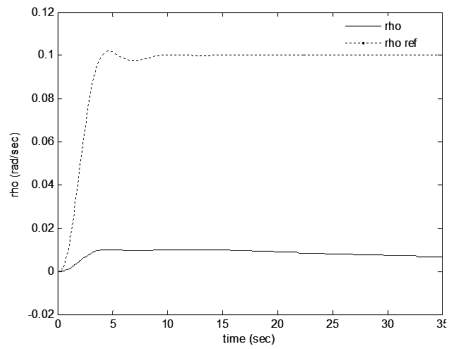

Figure 21. $K_E = 1000$, $K_{CE} = 100$, $K_U = 2\pi/180$.

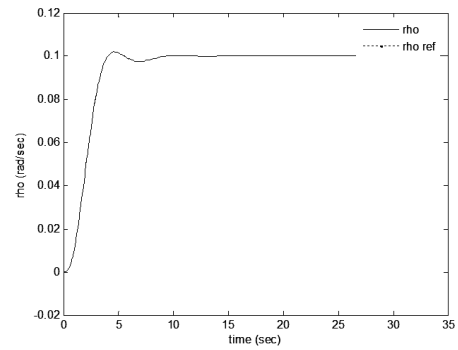

Figure 22. $K_E = 1000$, $K_{CE} = 1$, $K_U = 7\pi/180$.

The effect of variation of K_U on stability and steady state error of directional response when $K_E = 1000$ and $K_{CE} = 1$ in a smooth lane change maneuver is shown in Tab. 9 and from Fig. 22 to Fig. 26. For $K_U = 2\pi/180$, the directional response perfectly tracks the yaw rate command with 99.99% accuracy. For $K_U = (n\pi/180)$ for $n = 0.5, 1, 2, 3, 6, 7, 8, 10, 13, 14, 15, 16, 17, 18, 20$, the directional response also perfectly tracks the yaw rate command with 99.99% accuracy except $n = 10$ and 7 where some intermediate disturbance is noticed and very soon the disturbance is eliminated shown in Fig. 22. For $K_U = -\pi/180$ to $K_U = -4\pi/180$, the response is sluggish, negative initially with very low peak value of 5% to 10% of steady state value and gradually becomes zero with 100% steady state error shown in Fig. 23 and Fig. 24. For $K_U = (\pi/3)/180$ to $K_U = (\pi/10)/180$, the response is sluggish, with very low peak value of 20% to 2% of steady state value and gradually becomes zero with 100% steady state error shown in Fig. 25 and Fig. 26.

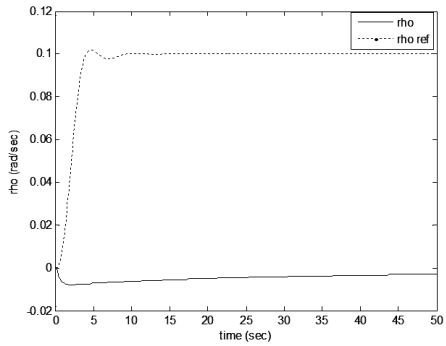

Figure 23. $K_E = 1000$, $K_{CE} = 1$, $K_U = -2\pi/180$.

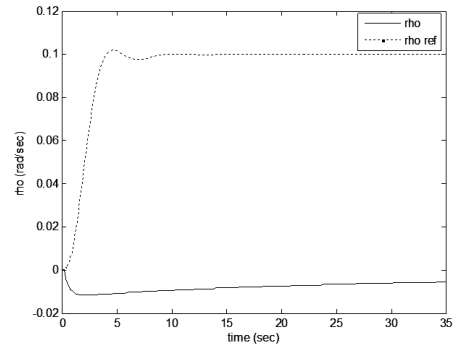

Figure 24. $K_E = 1000$, $K_{CE} = 1$, $K_U = -4\pi/180$.

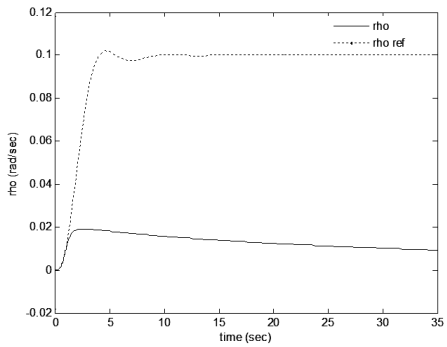

Figure 25. $K_E = 1000$, $K_{CE} = 1$, $K_U = (\pi/3)/180$.

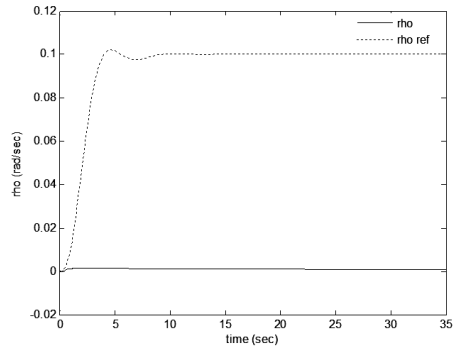

Figure 26. $K_E = 1000$, $K_{CE} = 1$, $K_U = (\pi/10)/180$.

4. Conclusion

This paper has presented two controllers namely PID and FLC for the directional control of a ground vehicle. The performances of the controllers have been evaluated while these are employed to control the vehicle's steering in a smooth lane change maneuver. From the results obtained it is observed that both the PID and FLC performed well in smooth lane change maneuver. The directional response of a ground vehicle has also been studied with FLC in a smooth lane change maneuver by varying scale factors like K_E, K_{CE} and K_U. From this response, the vehicle's explicit capabilities as well as its contribution to the system performance of the driver/vehicle combination can be obtained. Although PID controller exhibits slightly better dynamic performance but in the real-world scenario it is recommended to use fuzzy controller for this problem because accurate parameters of the vehicle may not be available for which PID may not be able to provide appropriate control whereas as FLC does not rely on vehicle parameters thus better performance can still be achieved using the latter.

In future, suitable yaw controller and speed controller can be designed in addition to directional controller, so that the entire vehicle state (ρ, υ, β) can be used to feedback to their respective controllers to aid steering or directional control.

References

[1] R. SEAKS, C.J. COX, J. NEIDHOEFER, P.R. MAYS and J.J. MURRAY: Adaptive Control of a Hybrid Electric Vehicle. *IEEE Trans. Intelligent Transportations*, **3**(4) (2002), 213-234.

[2] J. ACKERMANN: Robust decoupling, ideal steering dynamics and yaw stabilization of 4WS cars. *Automatica*, **60** (1994), 1761-1768.

[3] J. ACKERMANN and W. SIENEL: Roubst yaw damping of cars with front and rear wheel steering. *IEEE Trans. Control System Technology*, **CST-1** (1993), 15-20.

[4] T.D. GILLESPIE: Fundamental of Vehicle Dynamics. SAE, 1992.

[5] S.H. ZAK: Systems and Control. Oxford University Press, 2003.

[6] J. ACKERMANN: Robust car steering by yaw rate control. *Proc. of the 29th IEEE Conf. on Decision and Control*, Honolulu, Hawai, (1990), 2033-2034.

[7] E. ONO, S. HOSOE, H.D. TUAN and S. DOI: Robust stabilization of vehicle dynamics by active front wheel steering. *Proc. of the 35th IEEE Conf. on Decision and Control*, Kobe, Japan, (1996), 1777-1722.

[8] E. ONO, S. HOSOE, H.D. TUAN and S. DOI: Bifurcation in vehicle dynamics and robust front wheel steering control. *IEEE Trans. on Control Systems Technology*, **6**(3), (1998), 412-420.

[9] J.Y. WONG: Theory of Ground Vehicles. John Wiley & Sons, INC, New York, 2008.

[10] B. SUBUDHI and A.S. MORRIS: Fuzzy and neuro-fuzzy approaches to control a flexible single-link manipulator. *Proc. IM Es, Part I: J. Systems and Control Engineering*, **217** (2003), 387-399.

[11] B. HU, G.K.I. MANN and R.G. GOSINE: New methodology for analytical and optimal design of fuzzy PID controllers. *IEEE Trans. on Fuzzy Systems*, **7**(5), (1993).

[12] B. SUBUDHI and A.K. SWAIN: Genetic algorithm based fuzzy logic controller for real time liquid level control. *IE(I) Journal-EL*, (1996), 96-100.

[13] K.R.S. KODAGODA, W.S. WIJESOMA and E.K. TEOH: Fuzzy speed and steering control of an AGV. *IEEE Trans. on Control Systems Technology*, **10**(1), (2002), 112-120.

[14] B. SUBUDHI and S.S. GE: Sliding mode observer based adaptive slip ratio control for electric and hybrid vehicles. *IEEE Trans. Intelligent Transportations*, in press.

[15] P. KACHROO and M. TOMIZUK: Integral action for chattering reduction and error convergence in sliding mode control. *American Control Conference*, Chicago, USA, (1992), 867-870.

[16] E. ONO, K. TAKANAMI, N. IWAMA, Y. HAYASHI, Y. HIRANO and Y. SATOH: Vehicle integrated control for steering and traction systems by μ-synthesis. *Automatica*, **30**(11), (1994), 1639-1647.

[17] A.E. CETIN, M.A. ADLI, D.E. BARKANA and H. KUCUK: Implementation and development of an adaptive steering-control system. *IEEE Trans. on Vehicular Technology*, **59**(1), (2010), 75-83.

[18] T.L. LAM, H. QIAN and Y. XU: Omnidirectional steering interface and control for a four-wheel independent steering vehicle. *IEEE/ASME Trans. on Mechatronics*, **15**(3), (2010), 329-338.